Article

Indoor Thermal Environment in Different Generations of Naturally Ventilated Public Residential Buildings in Singapore

Ji-Yu Deng ![ORCID], Nyuk Hien Wong, Daniel Jun Chung Hii, Zhongqi Yu, Erna Tan, Meng Zhen and Shanshan Tong *

Department of Built Environment, National University of Singapore, Singapore 117566, Singapore
* Correspondence: tongshanshan117@gmail.com

Abstract: This study aims to evaluate and compare the indoor air velocities and thermal environment inside different generations of public residential buildings developed by the Housing and Development Board (HDB) of Singapore and analyze the impact of façade design on the indoor thermal environment. To achieve this goal, several case studies were carried out, namely, five typical HDB blocks built in different generations from the 1970s to recent years. Firstly, these five blocks with different façade design features were simulated to obtain the indoor air temperatures for both window-closed and window-open scenarios by using the EnergyPlus V22.2.0 (U.S. Department of Energy) and Design-Builder v6 software(DesignBuilder Software Ltd, Stroud, Gloucs, UK). Meanwhile, the computational fluid dynamics (CFD) simulations were conducted to obtain the area-weighted wind velocities in the corresponding zones to evaluate the indoor thermal comfort. Accordingly, the effects of façade design on indoor air temperatures under both the window-closed and window-open conditions were compared and analyzed. Positive correlations between the facades' window-to-wall ratio (WWR) and the residential envelope transmittance value (RETV) and T_a were confirmed with statistical significance at a 0.05 level. Furthermore, the indoor thermal comfort based on the wind open scenarios was also investigated. The results indicate that the thermal environment can be greatly improved by implementing proper façade design strategies as well as opening the windows, which could result in an average 3.2 °C reduction in T_a. Finally, some principles were proposed for the façade design of residential buildings in tropical regions with similar climate conditions.

Keywords: natural ventilation; thermal environment; computational fluid dynamics; residential building; window-to-wall ratio

1. Introduction

There are two types of residential buildings, including the public housing developed by the Housing and Development Board (HDB) and private condominiums developed by real estate developers, in Singapore. Approximately 93% of residents stay in either HDB flats or private housing such as condominium units [1]. In particular, the HDB public housing policy has benefited several generations of Singaporeans over the past few decades. So far, the public residential buildings developed by HDB have provided housings for more than 80% of Singapore's population. The HDB public housing policy currently covers 23 towns and 3 estates, as shown in Figure 1. According to statistics, there are more than 10,000 public residential buildings with in excess of 1 million units which accommodate Singaporeans for dwelling [2].

The comparison of these HDB residential buildings built in different generations shows that the design feature has evolved gradually throughout the years according to the market demands, feedbacks of residents, and the design trends in corresponding times. In addition to the simple types of public housing, such as the slab and point blocks, which had kept a dominant position in an earlier era, more complex floor plans have been presented since the 1990s. Moreover, the flat sizes show great diversities through the past few decades' developments even though the floor area of a single unit tends to

be smaller [3]. Thus, many different types of HDB flats have emerged, including 1-room, 2-room, 3-room, 4-room, 5-room, and executive flats, among which, the 3-room and 4-room HDB flats are the majority [1].
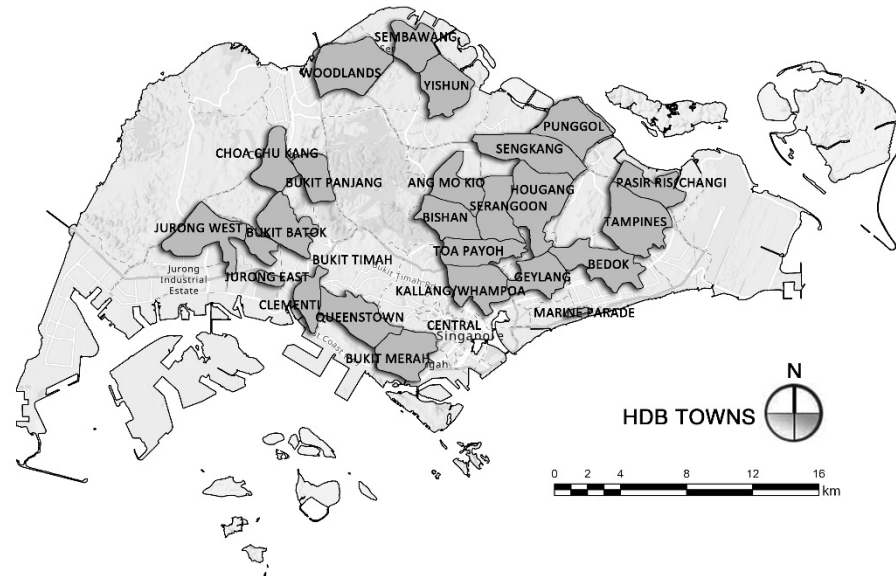
Figure 1. Locations of the HDB towns in Singapore.

Architectural design plays an important role in various kinds of buildings with occupancies. Especially for residential buildings, the design strategies not only affect the patterns of daily life and behavior of the residents, but also the indoor thermal environment, such as the indoor air temperature and thermal comfort [4].

This study aims to compare the vertical façade design strategies between different generations of HDB residential buildings and investigate the impacts of façade design parameters on the indoor air temperature and the thermal comfort under natural ventilated conditions. For the comparative analysis, all the HDB residential buildings built from the 1970s to the present are classified into 5 generations totally according to the built years and locations. A comparison shows that each generation has its features which allows it to be identified easily from the complex building cluster in the urban context. Thus, several typical HDB blocks are selected as case studies which are presented in this paper to explore the relationship between façade design strategies and the indoor thermal environment.

2. Literature Review

The influence of building façade design on indoor wind and thermal performance is usually caused by the façade orientation, window opening, and the availability of shading devices. Givoni initially launched the study on the optimization of a multi-story building's plan by employing wind-induced ventilation under the hot humid climate, which proposes that the building's orientation needs to be oblique to the prevailing wind [5]. He also demonstrated that the window orientation has minor effects on the indoor temperatures of effectively ventilated buildings [6]. A case study in Chongqing conducted by Costanzo et al. also found that the average amount of air change rates varies in a large range by changing the windows orientation [7]. However, the façade orientation mentioned in above studies all refers to the windward side façade, which is generally more effective in affecting the indoor wind and thermal environment in comparison to the leeward side.

As for the window openings configuration, it usually involves the area and position of windows. As a common indicator of window area, window-to-wall ratio (WWR) is also a key parameter determining the amount of incident solar radiation entering the interior. In the Singapore context, a large value of WWR often leads to higher solar heat gains during the daytime and facilitates heat dissipation at night under natural ventilation. Hence, it is

crucial to explore whether there is an optimal WWR for buildings. Givoni found that the effect of window size on the indoor wind condition is approximately proportional to the square root of the opening size by conducting a wind tunnel study on a square model [6]. Wang and Wong found that ventilation and indoor thermal comfort could be dramatically enhanced by 13% with the increase of WWR from 12% to 24% in the hot–humid climate of Singapore [4]. The effects of WWR on building energy demands were also explored and documented in several studies, and some of these studies were carried out to establish guidelines for energy-efficient architectural design [8–11]. Furthermore, several previous studies examined the performance of window position and highlighted its significance in affecting the wind and thermal environment in natural ventilated buildings [7,12–14]. The outcomes of these studies validated that choosing the right position and orientation would greatly benefit natural ventilation and improve the indoor thermal comfort.

As an accessory to the façade openings, the external shading devices are designed not only to avoid overheating, but also to provide significant impact towards improving indoor thermal conditions [15,16]. They could be classified into three basic forms, horizontal overhangs, vertical side fins, and combinations of horizontal and vertical. The geometries can be customized following the seasonal sun path. The studies launched by Wong et al. and Yang et al., respectively, showed that indoor air temperature reductions of 0.61–0.88 °C and 0.98 °C could be achieved with proper installation of external shading devices [17,18]. Besides, the potential of shading devices in cooling energy-saving and thermal comfort improvement has also been well recorded in many studies [17–22].

According to previous studies, obvious relationships can be concluded between façade design parameters and the thermal performance and natural ventilation as well as energy consumption in buildings. Studies have also shown tremendous improvement in the indoor thermal environment and saving in energy consumption by implementing passive design strategies. Especially for Singapore, which is situated close to the equator with relatively high temperature and humidity, it is crucial and necessary to develop and apply the passive design strategies in line with satisfactory thermal performance. The authorities also have recognized that the achievement of a comfortable indoor environment is greatly determined by the thermal performance of the building façade. Therefore, both HDB blocks and condominiums need to have the thermal performance of building facades assessed by residential envelope transmittance value (RETV) in Green Mark for Residential Buildings (GMRB2016) [23] as well as Building Control (Environmental Sustainability) Regulations since 2008. However, the truth is that although HDB flats and most of the condominium units are designed to be naturally ventilated, the usage of air-conditioning has been increasing. From the household energy consumption survey in 2017, 83% of house owners have air-conditioners [24]. One possible reason is that the RETV code was developed from a building cooling energy efficiency perspective. Therefore, it may fail to quantify the significance of the façade parameter on indoor thermal comfort when windows are open.

Based on the above literature review, although extensive studies have been conducted on naturally ventilated residential buildings, the existing knowledge on the relevant field is still insufficient. Firstly, most previous studies focused on a certain type of block shape or building floor plan. Furthermore, few studies have been conducted on the passive design of residential buildings built in different generations, except for a recent study carried out in the warm temperate climatic zone of Iran [25]. Thus, it is still necessary to dedicate more efforts to the indoor wind and thermal performance of architectural design factors of natural ventilated residential buildings in the tropical climate region. Accordingly, this study firstly analyzed the impact of façade design based on various block shape and floor plan, then investigated the typical façade design as well as its performance in different generations of residential buildings in the tropical climatic zone of Singapore. Thirdly, the relationship between the building thermal code (RETV) and air temperatures under both window open and closed scenarios is discussed.

3. Methodology

3.1. Local Climate of Singapore

The local climatic characteristics usually rank as the first among various factors which affect the indoor thermal environment in naturally ventilated buildings. Singapore is situated on the 1.2° N and 104° E and characterized by a tropical climate with relatively high temperature and humidity. The air temperature (T_a) ranges from the minimum of 23 °C to 25 °C during the nighttime to the maximum of 31 °C to 34 °C during the daytime. As shown in Figure 2, based on the climate data from 1981 to 2010 [26], Singapore has quite high and uniform dry-bulb air temperatures throughout the year. The differences are less than 2.1 °C, 1.5 °C and 1.9 °C in the daily maximum, daily minimum and monthly mean dry-bulb temperatures among the 12 calendar months. Since Singapore is near the equator, the length of its day and the amount of sunshine it receives are relatively constant throughout the year as well. Daily sunshine hours are mainly influenced by the presence or absence of cloud cover. The daily sunshine duration with direct irradiance from the sun of more than 120 W/m^2 ranges from 4~5 h during the wettest months to 6~7 h during the drier periods [27]. The relative humidity (RH) is quite uniform throughout the year with an average of around 84%. The monthly rainfall for Singapore ranges between 112.5 mm and 320 mm with an average of 180 mm, while the average monthly wind speed ranges from 1.5 m/s to 3.1 m/s. According to the data records of the National Environment Agency (NEA), the prevailing winds are mainly from south, north, and two intermediate directions of southeast and northeast.

Although Singapore has hot and humid climate conditions throughout the year, successful building layout and façade designs and effective ventilation strategies could provide an optimum modifier to achieve a better indoor thermal environment. Therefore, the case studies should be conducted under the weather condition of a typical sunny day for a better understanding of the relationships between the building design features and indoor thermal conditions. Based on the comparison of the daily weather profiles of the typical meteorological year (TMY) of Singapore, the weather data on 30 April with the daily peak air temperature reaching 33.3 °C were used as the background weather file for the indoor air temperature simulation (Appendix A Table A1).
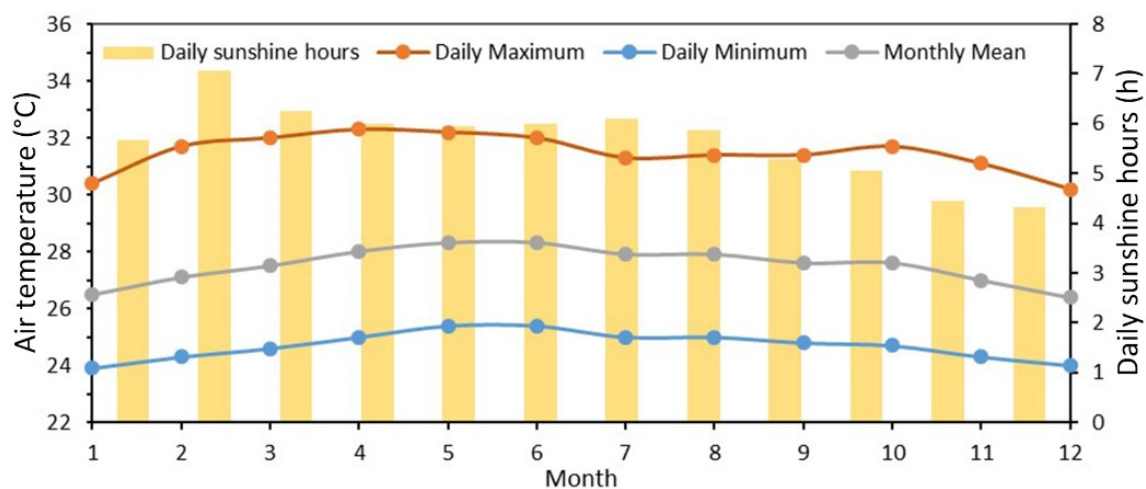
(**a**) Air temperature and sunshine hours

Figure 2. *Cont.*

(**b**) Wind speed and rainfall
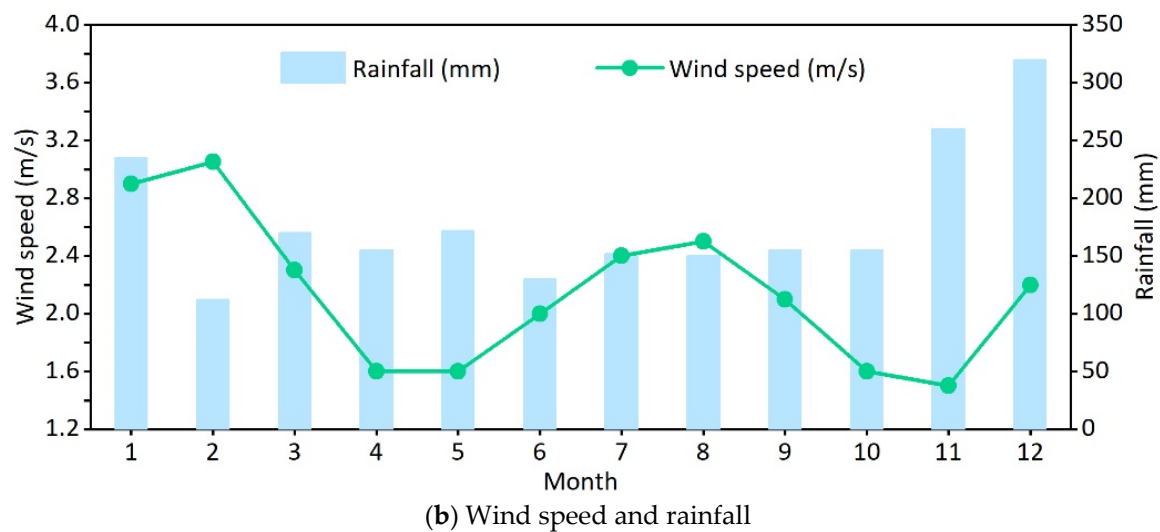
Figure 2. Monthly variations of meteorological variables in Singapore: (**a**) air temperature and sunshine hours; and (**b**) wind speed and rainfall.

3.2. Selecting Typical Flats for Different Generations of HDB Residential Buildings

According to the statistics of total built HDB flat units in all the HDB towns and estates, some representatives of HDB blocks with typical flats corresponding to different generations were selected for evaluation. Firstly, the HDB towns were classified into generations of the 1970s, 1980s, 1990s, 2000s, and 2010s according to their built years. As a result, 5 HDB towns with the largest number of total flat units were selected as the representative HDB towns for above 5 generations. Then, the flat type with the most units was selected as the typical flat for each representative HDB town. Table 1 shows the statistics of the representative HDB towns with the typical flats.

Table 1. Representative HDB towns with typical flat types for case study.

Generation	HDB Town	New Town/Estate	Flat Type	Total Flat Amount
1970s	Ang Mo Kio	Ang Mo Kio New Town	3-room	24,575
1980s	Tampines	Tampines New Town	4-room	24,046
1990s	Sengkang	Sengkang New Town	4-room	27,684
2000s	Punggol	Punggol New Town	4-room	16,613
2010s	Yishun	Yishun New Town	4-room	4722

Finally, the HDB block with the largest number of typical flats was picked out in each corresponding HDB town for different generations. As a result, these 5 blocks were selected as the exampling cases for investigation respectively. For privacy protection, these 5 blocks were named AMK (Ang Mo Kio), TP (Tampines), SK (Sengkang), PE (Punggol East), YS (Yishun) instead of the actual block IDs. The typical flat units at the mid-story of the target buildings were selected as the target units for investigation (Figure 3). The story numbers and the floor heights of the target units are listed in Table 2.

(**a**) Block AMK

(**b**) Block TP

(**c**) Block SK
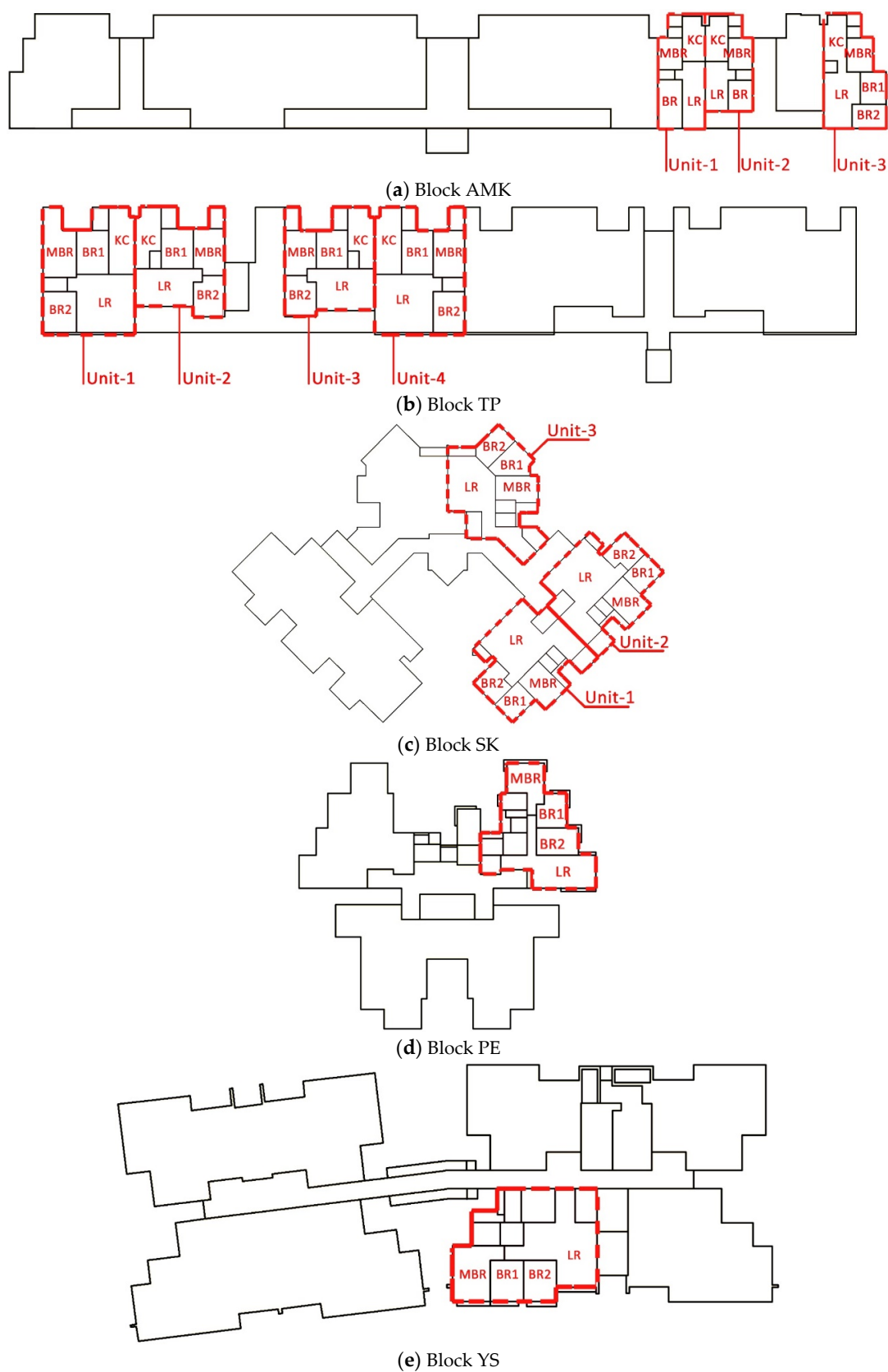
(**d**) Block PE

(**e**) Block YS

Figure 3. Locations of the target units on the standard floors of the target buildings: (**a**) block AMK; (**b**) block TP; (**c**) block SK; (**d**) block PE; and (**e**) block YS.

Table 2. Total story numbers and building heights of the target units.

Target Building	Total Stories	Building Height (m)	Target Units' Story	Target Story Height (m)
AMK	13	36.7	7	17.1
TP	13	36.7	7	17.1
SK	17	49.4	9	23.2
PE	19	54	9	23.2
YS	13	38.2	7	17.6

For a better understanding of the relationship between façade design and the indoor thermal environment, some façade design features of the target units are investigated and compared, including the façade orientation, WWR, RETV, and the depth of shading. These features are listed in Table 3 corresponding to 5 different generations respectively.

Table 3. Façade design parameters of the target units.

Unit	Zone	Orientation	WWR	Depth of Shading	RETV (W/m^2)	Adjacent to Corridor
AMK1	LR	S	0.3	200 mm	15.15	No
	KC	N	0.4	200 mm	16.83	No
	BR	S	0.3	200 mm	15.15	No
AMK2	LR	S	0.2	200 mm	13.10	Yes
	KC	N	0.4	200 mm	16.83	No
	BR	S	0.2	200 mm	13.10	Yes
AMK3	LR	S	0.4	200 mm	17.21	No
	KC	N	0.4	200 mm	16.83	No
	BR1	E	0	No	4.59	No
	BR2	E	0	No	4.59	No
	MBR	E	0	No	4.59	No
TP1	BR2	S	0.3	400 mm	14.59	No
	BR2	W	0	No	7.04	No
	MBR	W	0.1	No	21.51	No
TP2	LR	S	0.3	400 mm	14.59	Yes
	BR2	S	0.3	400 mm	14.59	Yes
TP3	LR	S	0.3	400 mm	14.59	Yes
	BR2	S	0.3	400 mm	14.59	Yes
TP4	LR	S	0.4	400 mm	16.46	No
	BR2	S	0.3	400 mm	14.59	No
SK1	BR1	SW	0	No	11.32	No
	MBR	SE	0.1	400 mm	13.35	No
SK2	BR1	NE	0	No	11.32	No
	MBR	SE	0.1	400 mm	13.35	No
SK3	BR2	NE	0.3	400 mm	17.42	No
	MBR	E	0.1	400 mm	13.97	No
PE	LR	S	0.5	850 mm	18.57	No
	BR2	E	0.3	350 mm	19.11	No
	MBR	N	0.6	350 mm	21.69	No
YS	LR	S	0.5	300 mm	20.41	No
	BR1	S	0.5	300 mm	20.41	No
	BR2	S	0.4	300 mm	18.58	No
	MBR	W	0.5	300 mm	20.41	No

It is necessary to note that the RETV is an important parameter for evaluating the thermal performance of the residential building's facades. According to GMRB2016, the

RETV of all the buildings should not exceed a maximum of 25 W/m^2 [23]. The RETV can be calculated through Equation (1):

$$RETV = 3.4(1 - WWR)U_w + 1.3(WWR)U_f + 58.6(WWR)(CF)(SC) \tag{1}$$

where WWR is the window-to-wall ratio (fenestration area/gross area of the exterior wall), U_w is the thermal transmittance of the opaque wall (W/m^{2}K), U_f is the thermal transmittance of fenestration (W/m^{2}K), CF is the correction factor for solar heat gains through fenestration, SC is the shading coefficient of fenestration.

3.3. Air Temperature Simulation with EnergyPlus and Design Builder Software

To fulfill the assessment and comparative analysis on the indoor thermal environment, the T_a in different habitable spaces of the target units was simulated by employing the EnergyPlus and Design Builder software according to the collected drawings and materials information. As mentioned before, the weather data on 30 April of TMY of Singapore were used as the background weather file for calculation. Moreover, note that the upper and lower floors of the target units were also modeled to avoid any influence from the ceiling or floor to the target units. To eliminate the impact of human activities on indoor air temperature and focus on the impact of façade design, the occupancy density and internal load due to lighting were set to zero. In addition, the simulations were conducted under both window-closed and window-open scenarios. The ACH rate was set to 80 to represent the ideal indoor natural ventilation mode under the window-open scenario.

The thermal and radiation properties of building envelopes were designed in accordance with the floor plan of each block and common thermal properties of public housing blocks. In general, the external wall was made of 30-cm reinforced concrete, and the internal wall was made of 10-cm reinforced concrete. The window glass was made of 8-mm grey glass. The properties of wall and glass materials are listed in Table 4.

Table 4. Thermal and radiation properties of façade materials.

	Material	Conductivity (W/mK)	Specific Heat (J/kg K)	Density (kg/m^3)	Solar Absorptance
Wall	Reinforced concrete	2.3	1000	2300	0.6

	Material	Solar heat gain coefficient (SHGC)		U-value (W/m^2 K)	
Glass	Grey glass	0.71		5.5	

3.4. Obtaining Wind Velocity with CFD Simulation

In addition to the air temperatures obtained in various habitable spaces of the target units, the area weighted air velocities in the corresponding zones are also required for evaluating the indoor thermal comfort. In this study, CFD simulations were conducted to all the representative cases by Ansys Fluent v19.0 (Ansys, Inc., Canonsburg, PA, USA). For the convenience of comparative analysis, we chose to simulate the single building rather than the residential community. Meanwhile, all the walls were assumed to be without thickness to simplify the calculation. To ensure the quality and accuracy of the results, the following settings and algorithms were applied.

3.4.1. Computational Domain and Grids Generation

The target buildings were included in a cuboid computational domain. The domain size was set according to the relevant best practice guidelines [28] based on the Architectural Institute of Japan (AIJ) & European Cooperation in Science and Technology (COST) guidelines [29,30]. In general, the outlets are set to be at least 15H$_{max}$ away from the group of explicitly modeled buildings, while the inlet, lateral, and top boundaries of the

computational domain are usually set to be at least $5H_{max}$ away from it. H_{max} is the height of the tallest building in each of the domains. It is necessary to note that all the four prevailing wind directions in Singapore, including north, northeast, south, and southeast, were required to be considered in the CFD simulations based on GMRB2016 [23]. The requirements were made based on the statistics of 18-year data from Changi climate station observed by NEA. Accordingly, the most prominent winds in Singapore are mainly from the north and northeast during the Northeast Monsoon (December to March), and from the south and southeast during the Southwest Monsoon (June to September). The inter-monsoon months (April, May, October, and November) are transition periods between the monsoons and show lighter and more variable winds. Figure 4 shows the annual wind rose of Singapore [26]. Therefore, for the convenience of model settings, all the side boundaries were set to be $15H_{max}$ away from the group of explicitly modeled buildings for considering varying inflow wind directions from the reference height of 15.0 m (Figure 5).
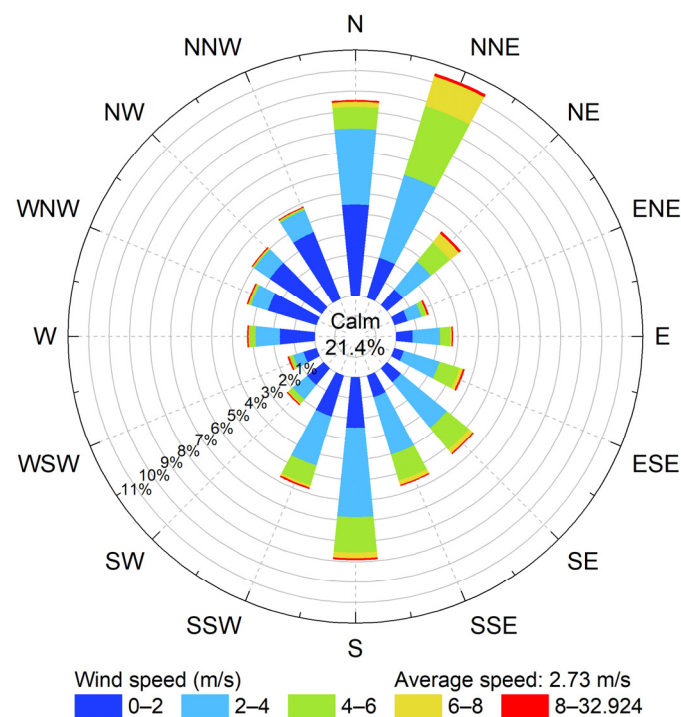

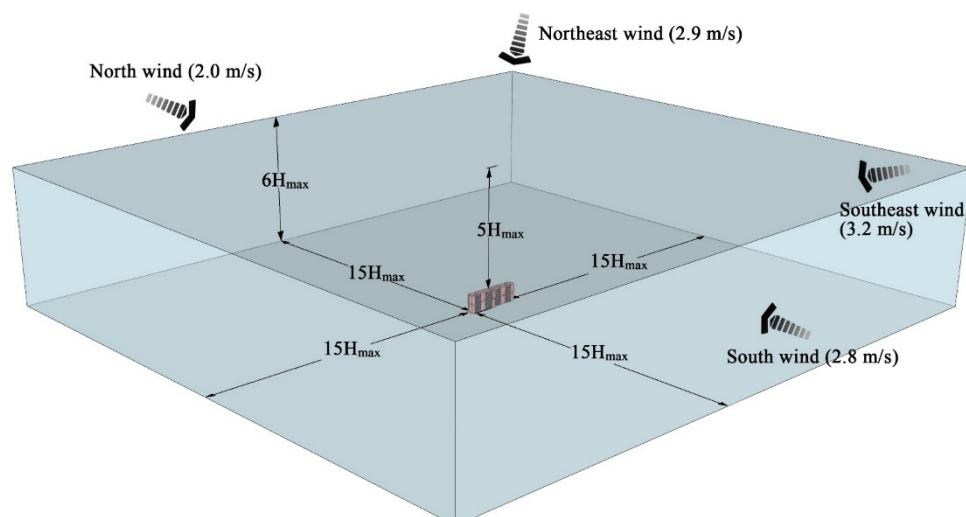**Figure 4.** Annual wind rose of Singapore.

Figure 5. Size of the computational domain and its relation to the buildings.

The computational grids were generated by employing Ansys Meshing 19.0. The proximity and curvature functions were chosen as the grid size control method. The minimum grid size was set to 0.005 m with a growth rate of 1.2 to control the cell size growing. The assembly meshing method employed the Cutcell technique. The inflation method for obtaining higher resolution around the building and external boundaries used the smooth transition of cell growth based on the minimum and maximum cell size. The generated meshes consist of 3.0 to 5.1 million unstructured cells with an average skewness below 0.05 and an average orthogonal quality above 0.95 corresponding to different target blocks, which means the mesh quality is good enough for the modelling.

The sensitivity test was done to understand the impact of grid size on velocity magnitude values captured. Including the minimum grid size of 0.005 m, five kinds of successive grids with various resolutions were applied in the case of block PE to validate the grid independence. The steps of mesh refining are illustrated in Table 5; the grid was refined and coarsened with a ratio no less than 2 in the minimum size.

Table 5. Total cell numbers of five consecutive grids.

No.	Grid Quality	Minimum Size (m)	Total Cell Numbers
1	Finest	0.005	3,058,596
2	Fine	0.02	2,477,176
3	Medium	0.05	2,018,771
4	Coarse	0.2	828,860
5	Coarsest	0.5	361,088

The influence of minimum grid size on the area-weighted wind velocity was evaluated by comparing the velocities obtained from 10 points of the indoor spaces near the windows at 25.2 m above ground level. The comparison between grid No. 1 and the other grid sizes shows slight differences, while the comparison between grid No.1 and the coarsest grid (No. 5) shows significant deviations (Figure 6). This confirms that the model with the minimum grid size below 0.2 m is sufficient to ensure the accuracy of simulation results. In consideration of the minimum dimension (0.1 m) of shading devices, the zero thickness walls, and the affordable simulation time, grid resolutions with minimum size of 0.005 m were applied in all the selected cases.
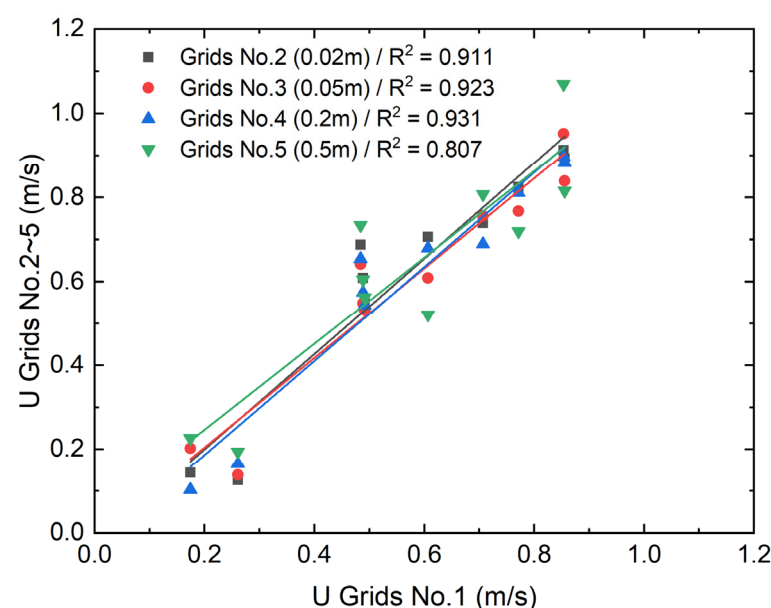
Figure 6. Comparison of the different grids concerning area-weighted wind velocity.

3.4.2. Boundary Conditions

According to the requirements of GMRB2016, the boundary conditions were set as follows. First of all, a logarithmic law (Equation (2)) was applied to the inlet to provide the vertical wind speed profile. The turbulent kinetic energy (k) and turbulence dissipation rate (ε) profiles were defined by Equations (3) and (4) given by Richards and Hoxey [31]:

$$U(z) = \frac{u^*}{\kappa} \ln \frac{z + z_0}{z_0} \tag{2}$$

$$k = \frac{u^{*2}}{\sqrt{C_\mu}} \tag{3}$$

$$\varepsilon = \frac{u^{*3}}{\kappa(z + z_0)} \tag{4}$$

where z (m) is the height coordinate, z_0 (m) the aerodynamic roughness length (given as 0.5 m in this study), κ the von Karman constant (usually given as 0.42), C_μ the model constant (generally given as 0.09), and u^* (m/s) the atmospheric boundary layer (ABL) friction velocity, which is defined by Equation (5):

$$u^* = \frac{\kappa U_{ref}}{\ln\left(\left(z_{ref} + z_0\right)/z_0\right)} \tag{5}$$

where U_{ref} is the reference wind speed at the reference height (z_{ref}) of the inlet wind speed profile. Based on the requirements of GMRB2016, wind environment CFD simulations should be conducted based on the assumption of four prevailing winds at a reference height (z_{ref}) of 15 m as the reference wind speed (U_{ref}), including the north, northeast, south, and southeast wind direction with respective speeds of 2.0 m/s, 2.9 m/s, 2.8 m/s, and 3.2 m/s, as shown in Figure 5 [23]. Accordingly, the wind speed profiles for inlet boundary could be mathematically described by log law functions with $z_0 = 0.5$ m.

For the outlet, lateral, and top boundaries, the conditions of natural outflow and free slip were utilized. In addition, the standard wall functions by Launder and Spalding [32] were applied to the ground surface in combination with the roughness modification by Cebeci and Bradshaw [33]. The roughness height (k_S) and roughness constant (C_S) were defined by using Equation (6) with the aerodynamic roughness length z_0. These values were given as $k_S = 0.7$ m and $C_S = 7$ in this study. Moreover, the standard wall functions were also applied to the building surfaces with $z_0 = 0.004$ m, and the values were given as $k_S = 0.0783$ m and $C_S = 0.5$.

$$k_S = \frac{9.793 z_0}{C_S} \tag{6}$$

3.4.3. Solver Settings

In this study, the 3d steady RANS equations (Equations (7)–(9)) were solved with the realizable k-ε turbulence model [34] owing to the excellent performance for wind field around buildings [35] and indoor wind flow [36,37]. The pressure–velocity coupling modelling was performed by using the SIMPLE algorithm, and the second-order discretization schemes were utilized for all the convection and viscous terms of the governing equations. Furthermore, the convergence standard was set to be that all the scaled residuals, including the x, y, and z velocity, k and ε, and continuity, reaching at least 10^{-4} smoothly without any significant oscillations.

$$\frac{\partial U_i}{\partial X_i} = 0 \tag{7}$$

$$\frac{\partial U_i}{\partial t} + U_j \frac{\partial U_i}{\partial X_j} = -\frac{1}{\rho} \frac{\partial P}{\partial X_i} + \frac{\partial}{\partial X_j} \left(2\nu S_{ij} - \overline{u'_j u'_i} \right) \tag{8}$$

$$S_{ij} = \frac{1}{2}\left(\frac{\partial U_i}{\partial X_j} + \frac{\partial U_j}{\partial X_i}\right) \tag{9}$$

In these equations, U_i and U_j are the mean velocities in X_i and X_j directions, P the mean pressure, t the time, ρ the density, ν the molecular kinematic viscosity, u'_i and u'_j the fluctuation components, and S_{ij} the strain-rate tensor. The horizontal bar represents the mean value.

3.4.4. Validation of the CFD Solver with the Realizable k-ε Turbulence Model

The study by Ramponi and Blocken [38] was selected for comparative validating of the CFD solver with the realizable *k-ε* turbulence model employed in this paper. The reference study was conducted on a generic isolated building using the Fluent 6.3 solver with various turbulence models and different total mesh counts. The results of the reference study were validated by a detailed particle image velocimetry (PIV) measurement of wind-induced cross-ventilation for generic isolated building models conducted by Karava et al. [39]. For the CFD validation, an equivalent computational grid of 605,888 hexahedral cells was generated with a stretching ratio of 1.2 to match the mesh result of the reference study, which has 575,247 hexahedral cells (Figures 7 and 8). The boundary conditions used in their study are strictly followed to replicate the same performance using Fluent 19.0.
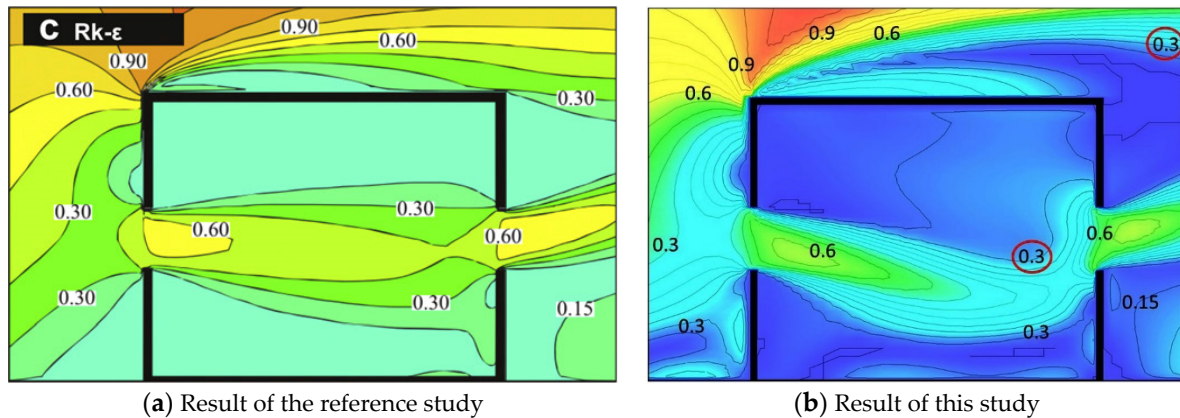

(**a**) Mesh result of the reference study　　　　　(**b**) Mesh result of this study
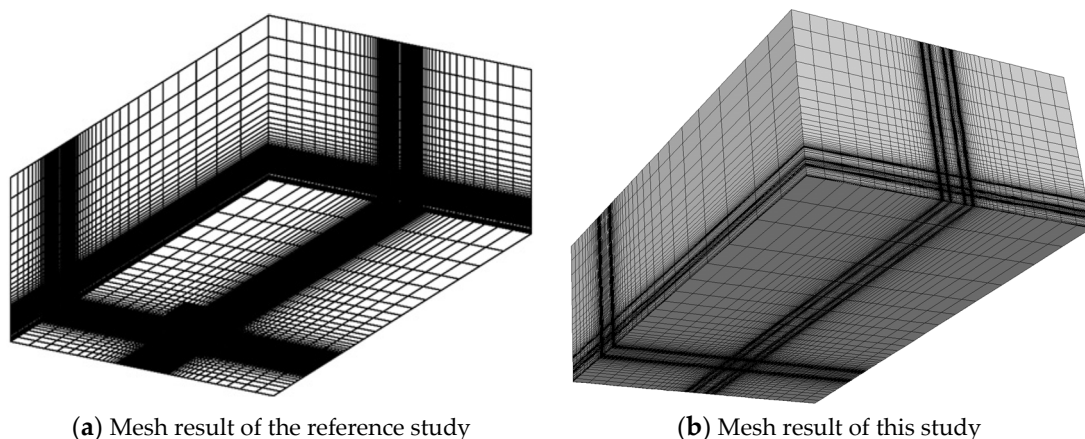
Figure 7. Perspective view of the grid at the bottom, side, and back face of the computational domain: (**a**) mesh result of the reference study; and (**b**) mesh result of this study.

(**a**) Mesh result of the reference study　　　　　(**b**) Mesh result of this study
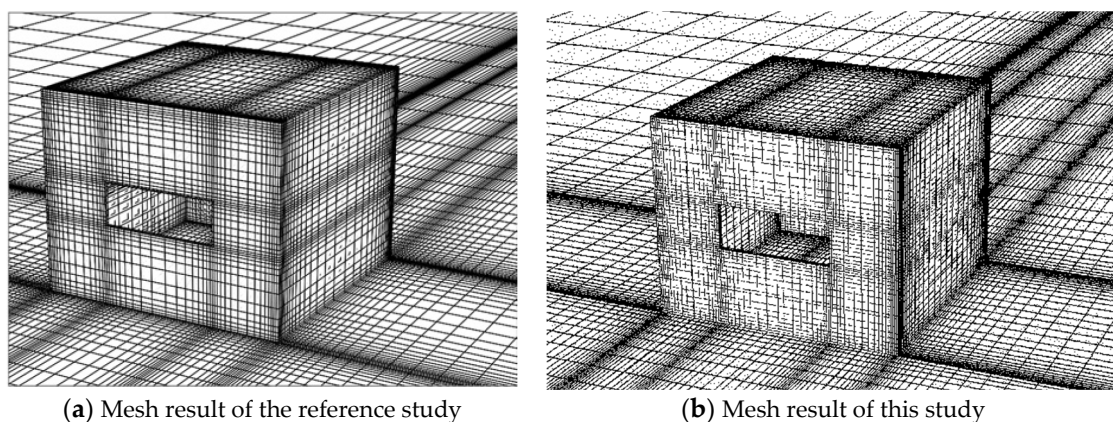
Figure 8. Perspective view of the grid at building surfaces and ground surface: (**a**) mesh result of the reference study; and (**b**) mesh result of this study.

Figure 9 shows the comparison of the contours at the vertical center plane around the building between the results from the reference study and this study. The wind velocity

ratio values are generally quite similar except the flow through the windward opening slightly bends downwards before going through the leeward opening. In addition, the value at the leeward side of the roof is lower. Nevertheless, the wind velocity ratio and flow pattern are almost identical to the one validated.

(a) Result of the reference study   **(b)** Result of this study

Figure 9. Wind speed ratio contours in the vertical center plane: (**a**) result of the reference study; and (**b**) result of this study. The red/orange colors in the figures represent higher wind speed ratios and blue/green colors represent lower wind speed ratios. The values with red circles indicate the disparities between (**a**,**b**).

Regarding the disparities between the results of the reference study and this study, it is possibly owing to the different solver versions used as well as the missing details of the minimum and maximum cell sizes. Nonetheless, it is reasonable to regard that the discrepancies could be considered negligible and acceptable, and the solver settings are credible to be applied in this study.

3.5. Indoor Thermal Comfort

In general, the indoor thermal comfort is related to the air temperature, wind speed, and relative humidity of the indoor environment. However, the relative humidity in Singapore shows a fairly uniform pattern throughout the year and normally keeps a high level around 83.9%. Given the uniformity and the stability of relative humidity throughout the year in Singapore, the indoor thermal comfort is mainly affected by the air temperature and wind speed under the window-open condition. Therefore, the thermal comfort in the naturally ventilated HDB blocks was evaluated based on the results of the hourly indoor air temperature simulation under the window-open scenario on the typical sunny day (30 April) from the EnergyPlus simulation, as well as the average indoor wind speed under four prevailing wind scenarios from the CFD simulation.

Accordingly, the empirical Predicted Mean Vote (PMV) model developed for the residential buildings in Singapore based on the local climate conditions was employed in this study to predict the thermal comfort index in the studied HDB rooms, as given in Equation (10) [23]:

$$PMV = -11.7853 + 0.4232T_a - 0.57889v \tag{10}$$

where PMV is the predicted mean vote, T_a is the indoor air temperature (°C), and v is the indoor wind speed (m/s). The PMV corresponds to residents' thermal sensation on a seven-point scale from cold (−3) to hot (+3).

It is necessary to note that this model is only applicable for the window-open scenario since the indoor wind speed is available under natural ventilation condition. It is also worth noting that for the thermal comfort evaluation, the indoor air temperature and wind results were simulated separately in this study, rather than using a coupled thermal/airflow simulation, due to the advantages of EnergyPlus in indoor air temperature simulation and

the CFD technique in airflow simulation separately under various scenarios (e.g., hourly outdoor weather conditions, prevailing winds, window openings).

4. Results and Discussion

4.1. Air Temperature (T_a)

4.1.1. Window Closed Scenarios

Figure 10 shows the maximum daytime average and annual average T_a in various habitable spaces of all the target units under the window-closed condition. For the slab blocks AMK and TP, the flat units are located along the long axis (E–W) of the slab shapes. This type of plan layout tends to result in overheating in indoor spaces by direct solar radiations with slight hindrances. Furthermore, the excessive heat inside the indoor spaces cannot be dissipated because of the closed windows. Therefore, the T_a near the facades adjacent to the corridor (zone AMK2-LR, AMK2-BR, TP2-LR, TP2-BR2, TP3-LR and TP3-BR2) are lower than those near the facades nonadjacent to the corridor. This is because the facades adjacent to the corridor are mostly shaded by the corridor which could prevent excessive solar access while the facades nonadjacent to the corridor receive more direct solar radiations.
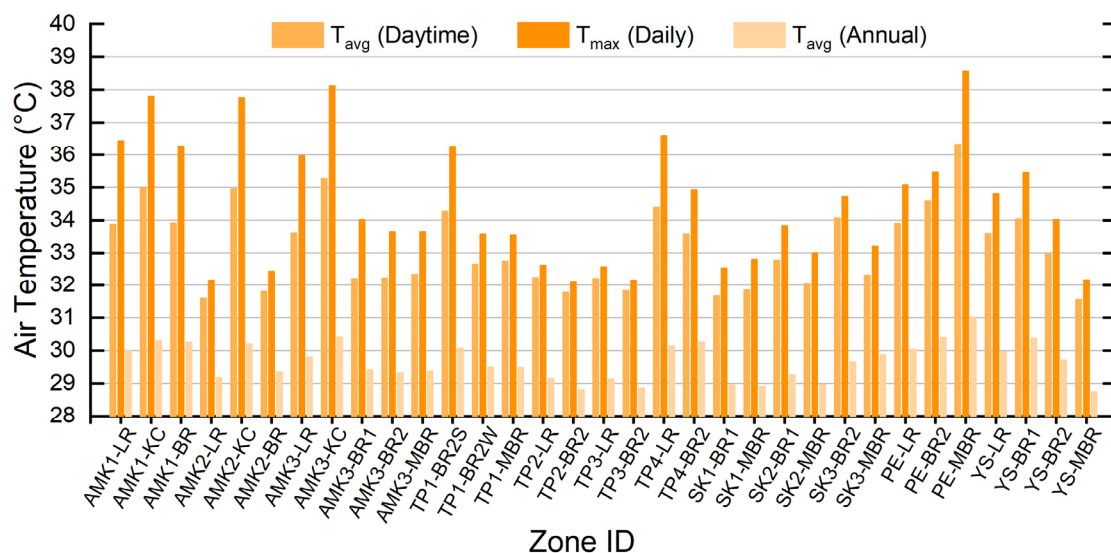
Figure 10. Average and maximum T_a in target zones for window closed scenario.

In addition, some exceptions can be found in 3 zones (AMK3-BR2, AMK3-BR1, and AMK3-MBR) in unit 3 of block AMK. The T_a in these zones are also much lower, even they are nonadjacent to a corridor. The possible reason for this phenomenon is that these locations are near to the east-facing facades without windows (WWR = 0). This kind of façade is more effective in preventing too much solar heat gains than the facades with large windows. Hence, the T_a near the south- and north-facing façades with large WWR (WWR = 0.4) in zones of AMK3-LR and AMK3-KC are higher. Similarly, the T_a near the west-facing facades (WWR = 0 and 0.1) of zones TP1-BR2 and TP1-MBR in the unit-1 of block TP are also lower than the T_a near the south-facing façade (WWR = 0.3) of zone TP1-BR2. This is much different from the circumstances in the regions with higher latitude in which the north-facing facades usually perform better in avoiding solar heat gains during the hot summer conditions. Apparently, the thermal performance of the façades in the regions near the equator, such as Singapore, usually depends on the WWR and depth of shading devices.

As for block SK, the T_a in most habitable spaces is also lower due to the small WWRs of the facades (WWR = 0 and 0.1) except for the zone of SK3-BR2 in which the façade WWR is 0.3. In contrast, the T_a in the habitable spaces with larger WWRs in block PE and YS is mostly higher. The highest T_a is observed near the north-facing façade of zone PE-MBR.

The possible reason for this behavior is that the largest window opening (WWR = 0.6) of this room could result in much more solar heat gains in the area near the windows.

However, the T_a in the area near the west-facing façade of zone YS-MBR is the lowest even though the WWR is 0.5. The possible reason for this behavior is that the west-facing façade is toward the cortile enclosed by the corridor and two blocks with significant shading conditions which cause the least solar heat gains in this part of zone YS-MBR. For the point and irregular blocks, the flat units are usually arranged circumferentially. Different parts of the blocks will provide certain shading conditions for each other. Thus, self-shading is also effective in reducing the heat accumulation caused by direct solar radiation.

4.1.2. Window Open Scenarios

The T_a in various habitable spaces of the target units under the window-open condition is shown in Figure 11. It can be seen that the T_a in all the rooms with opening windows is significantly lower than for those under the window-closed condition and is reduced by an average of 3.2 °C. This phenomenon mainly occurs due to the convenience of heat dissipation for indoor spaces under the window-open condition. It can be inferred that the natural ventilation produced by opening the windows could significantly facilitate the heat dissipation, and thus, the window-open scenarios have distinct potentials in cooling the indoor environment.
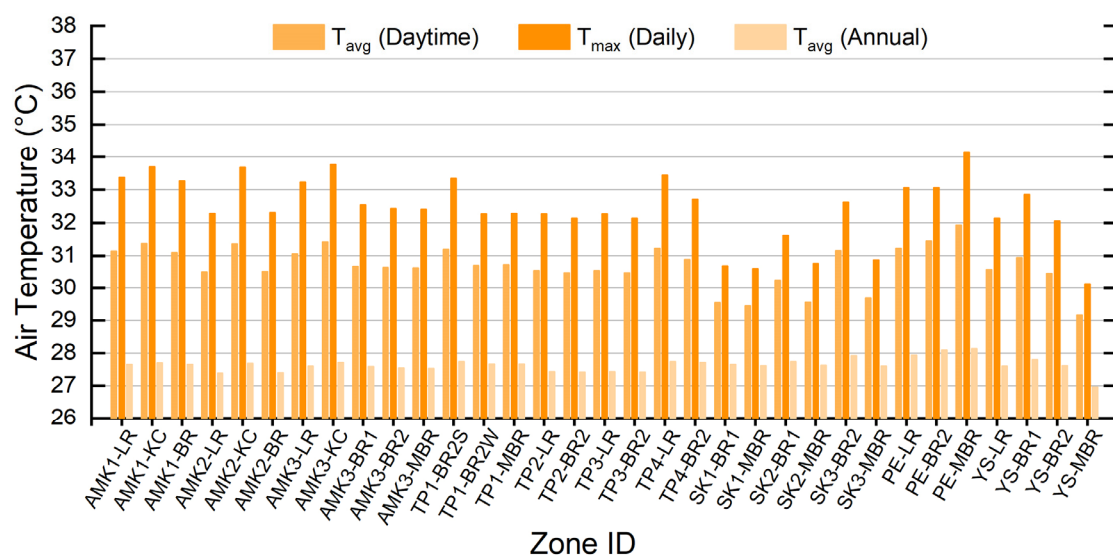
**Figure 11.** Average and maximum T_a in target zones for window open scenario.

Moreover, the T_a in different habitable spaces of the target units is much more identical under window-open condition in comparison to those in the window-closed scenarios. Especially for the annual average T_a, tiny differences could be observed between the annual average T_a obtained in different zones. This phenomenon happens mainly because the heat dissipation potentials under the window-open condition possibly result in the same cooling tendencies toward the ambient temperature.

Furthermore, due to the largest WWR of the north-facing façade of zone PE-MBR, the T_a near the façade is still the highest. In addition, the area near the west-facing façade of zone YS-MBR still holds a relative lower T_a under the window-open condition. Apart from the reason explained in the above section, the south-facing window opening also plays a role in releasing the interior heat gains.

4.1.3. Hourly T_a Profiles

Based on above analysis, both the shading condition and façade WWR are important in affecting the T_a. Especially for the shading condition provided by the corridor which is a crucial design feature for slab HDB blocks, it significantly benefits the daytime indoor ther-

mal conditions of slab blocks AMK and TP. However, the results show obvious differences in hourly T_a profiles between the window-closed and window-open scenarios, as shown in Figure 12.
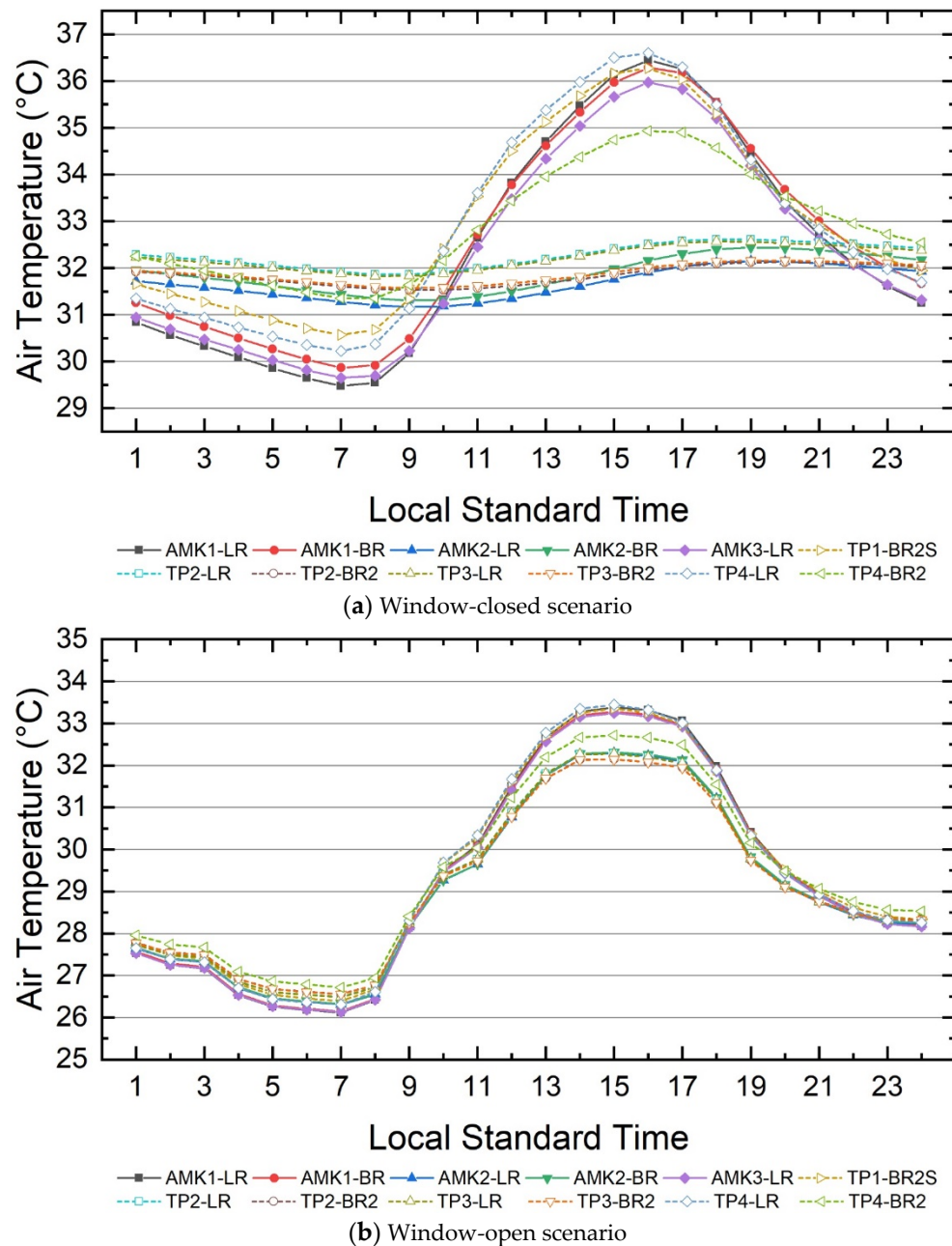
Figure 12. Hourly T_a profiles of all the target zones in blocks AMK and TP: (**a**) window-closed scenario; and (**b**) window-open scenario.

For the window-closed scenarios, the T_a in the zones adjacent to corridors are significantly lower than those in the zones nonadjacent to corridors from 10:00 to 22:00 while the situation reverses before 10:00 and after 22:00 (Figure 12a). The reason for this behavior is because the corridor could produce effective shading conditions during the daytime for avoiding excessive solar access to the spaces adjacent to it. On the contrary, the corridor could also obstruct the heat release during the night. It can be also observed that the hourly T_a profiles in the zones adjacent to corridors fluctuate greatly, while those in the zones adjacent to corridors are smoother. The difference of T_a reaches a maximum of 4.5 °C around 16:00. This phenomenon is possibly because of the buffering function produced by

the corridor, which could reduce the processes of heat convection and exchange between the interior and exterior environments.

However, the hourly T_a profiles in different zones tend to be convergent when the windows are open (Figure 12b), especially in the durations before 9:00 and after 22:00. The convergence of these T_a profiles is mainly because opening the windows could facilitate the heat convection and exchange between the inside and outside spaces and consequently minimize the discrepancy in T_a between different zones. Nevertheless, the corridor still plays an important role in preventing the rooms adjacent to it from excessive solar radiation. Especially during the noontime around 15:00, the difference of T_a between the rooms adjacent and nonadjacent to the corridor reaches the maximum of 1.3 °C. Thus, designing corridors in slab blocks has substantial potential in cooling the indoor spaces regardless of the windows' status.

4.2. Indoor Thermal Comfort (PMV)

The indoor thermal comfort in the naturally ventilated rooms in different generations of HDBs under window-open condition were evaluated using Equation (10), and the results are shown in Figure 13.
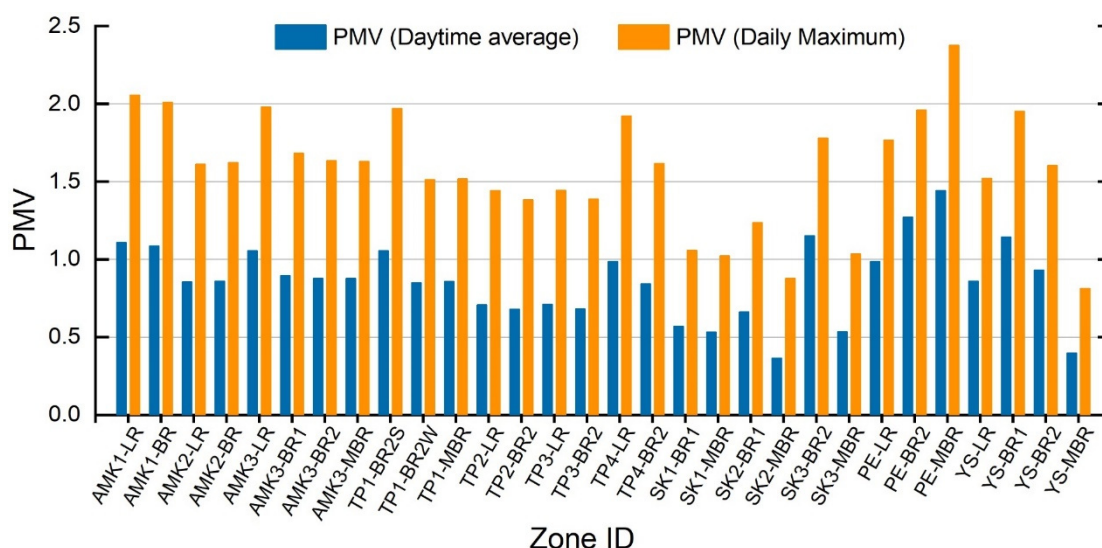

Figure 13. Average and maximum PMVs in target zones for window open scenario.

It can be seen that for the slab blocks (AMK and TP), the PMVs in the rooms adjacent to the corridor are generally lower than those nonadjacent to the corridor. This phenomenon confirms that the addition of the corridor could effectively improve the thermal comfort, although it may slightly reduce the indoor air velocity in cross-ventilated rooms. As for the blocks built in more recent decades, such as block SK, PE, and YS, the results of indoor thermal comfort show much greater variability. The possible reason for this behavior is their more complex designs such that the interior spaces are usually arranged in sequence to achieve better views and illumination. This kind of plan layout could result in the fact that the indoor air temperature and velocity are more sensitive to the façade orientation.

The highest daytime average and daily maximum PMVs are observed in the master bedroom of PE (PE-MBR). The reason can be explained as its largest WWR of 0.6 and highest indoor T_{max} among all the studied rooms. In comparison, the lowest daily maximum PMV appears in the master bedroom of YS (YS-MBR) despite its relatively large WWR of 0.5. The possible reason for this behavior is the cooling effect of self-shading provided by the neighboring block. In addition, most habitable spaces with the smallest WWRs of less than 0.3 in block SK hold relatively lower PMVs than the rooms in the other four blocks. This phenomenon validates the opinion that the most effective strategy to improve thermal comfort in tropical buildings is to reduce the solar heat gain with smaller WWRs.

4.3. Discussion

The façade design influences the natural ventilation potential of the HDB flat by many factors, such as the façade orientation, WWR, depth of shading, and so on. In this study, the impacts of WWR and shading depth were examined. Based on the façade surveys of different generations of HDB flats, the WWRs of the target units range from 0 to 0.4 in block AMK, TP, and SK which were built before the 2000s, while those of the target units in block PE and YS are mostly above 0.4 with a largest WWR reaching 0.6 that appeared in the north-facing façade of the master bedroom of block PE. Moreover, the shading depths of the bedrooms and living rooms increased from 20 cm to 85 cm over the decades. To evaluate the effects of building façade design parameters on the indoor wind condition, which is also a key variable for the indoor thermal comfort evaluation, it is necessary to employ the concept of the area-weighted wind velocity ratio (VR) to compare and analyze the indoor wind conditions between various habitable spaces under different prevailing winds. The *VR* can be calculated by Equation (11).

$$VR = \frac{V_{indoor}}{V_{incoming}} \tag{11}$$

where V_{indoor} is the wind speed in each habitable space, and $V_{incoming}$ is the incoming wind speed from the same level as the location of the corresponding target unit.

According to the results of average *VR* shown in Figure 14, it can be observed that the earlier generations of HDB flats perform better on natural ventilation than the later generations.
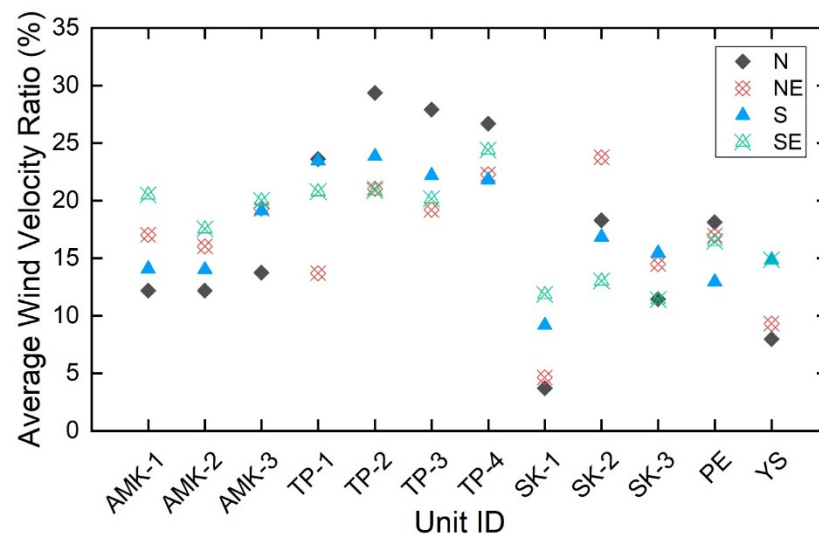

Figure 14. Average wind velocity ratios in all the target units.

However, the average *VR* in various habitable spaces does not always increase as the WWR increases and shading depth decreases as commonly intuited. Similar to the findings in a previous study in Singapore [40], the indoor air velocity could either increase or decrease as the WWR increases, depending on the relative sizes of the inlet and outlet, as well as the wind direction and facade orientation. Nevertheless, the results also confirm the complicated relationships between façade design parameters and the indoor air velocities as mentioned in previous studies [40–43]. Therefore, it is arbitrary to infer that the worse natural ventilation performance of the HDB block built after the 2000s is directly caused by the change of façade WWR and the depth of the shading device. Further investigations should be carried out by conducting a series of parametric studies before the exact conclusions come out.

To examine the impacts of façade design parameters on indoor air temperatures, a series of ordinary least square (OLS) regressions were conducted to test the relations

between the WWR and RETV of the studied facades and the daytime average T_a in the corresponding zones. For the convenience of comparative analysis, only the south-facing facades with windows were selected to be analyzed. The relationships between these two façade design parameters and average T_a in the corresponding zones under both window-closed and window-open conditions are shown in Figures 15 and 16. Some key indicators of OLS regression analysis are listed in Table 6.
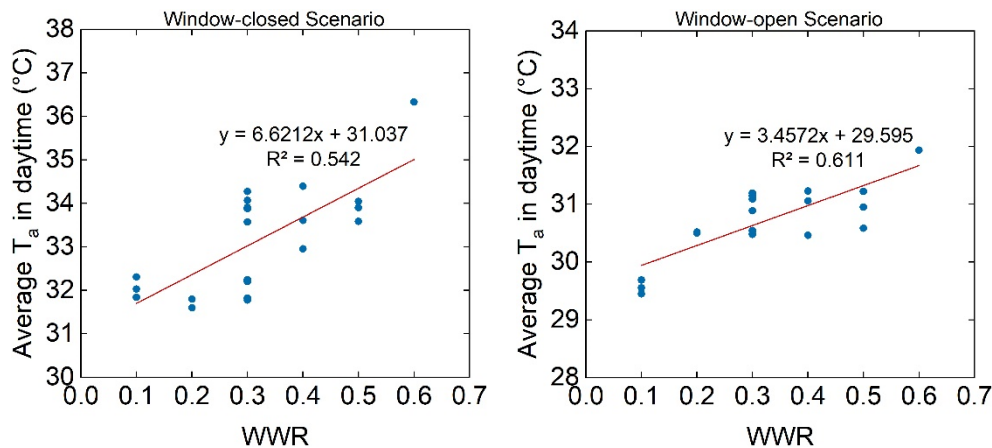

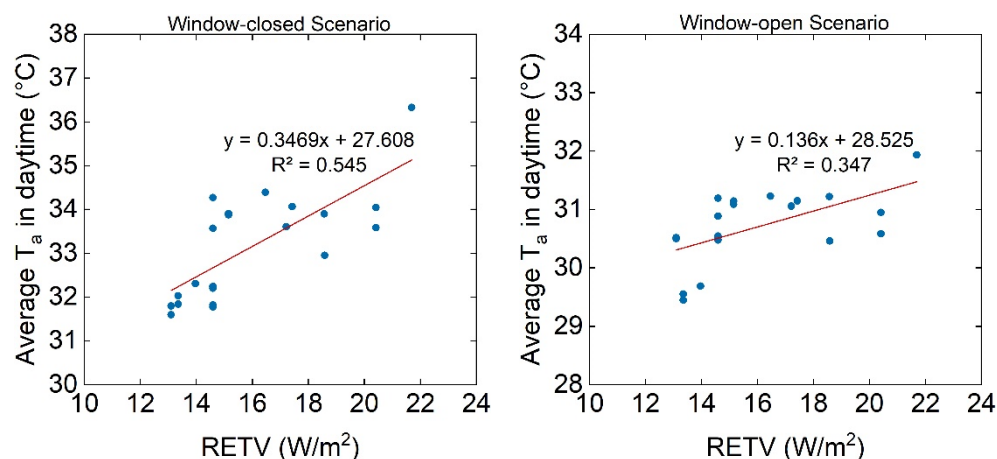**Figure 15.** Relationship between WWR and average T_a.

Figure 16. Relationship between RETV and average T_a.

Table 6. Key indicators of OLS regression analysis.

Independent Variable	Dependent Variable	Window Closed				Window Open			
		β	t	p	R^2	β	t	p	R^2
WWR	T_{avg} (Daytime)	6.621	4.739	0	0.542	3.457	5.459	0	0.611
RETV	T_{avg} (Daytime)	0.347	4.774	0	0.545	0.136	3.175	0.005	0.347

The results shown in the above figures indicate obvious positive relationships between these two facades design parameters and the average T_a in daytime regardless of the windows' status. The key indicators of OLS regression analysis listed in Table 6 show that both positive influences of WWR and RETV on the average T_a in daytime were confirmed with a statistical significance at the 0.05 level ($p < 0.05$).

Furthermore, according to the value of R^2, the linear correlation between WWR and the average T_a is almost identical to that between RETV and the average T_a under the window-closed condition. In comparison, the linear correlation between WWR and the

average T_a is more significant than that between RETV and the average T_a under the window-open condition. This phenomenon is possibly because the thermal transmittance value of the façade increases when the windows are open. It means opening the windows could change the RETV values of the façades. Thus, the linear correlation between the original RETV and the average T_a obtained in the window-open scenarios is weakened.

Nevertheless, it seems impossible to find and conclude a strong correlation between these two façade design parameters and the average T_a since the values of R^2 are mostly below 0.7. This is mainly caused by the variety, particularity, and complexity of the interior spaces in case studies. Further parametric studies on their correlations should be conducted to provide detailed and systematic analysis.

5. Conclusions

This study presents the assessment of the indoor thermal environment for the typical flat units of five different generations of HDB public residential buildings in Singapore. The results demonstrate that the building façade design play an important role in affecting the indoor air temperature and velocity, as well as the indoor thermal comfort. Based on the above analysis and discussions, some essential conclusions are drawn as below:

(1)　The comparison of the average T_a between the window-closed and window-open scenarios confirms that the window-open scenarios show greater potentials in cooling the indoor spaces in comparison to the window-closed scenarios. The maximum difference in T_a between the two scenarios reaches an average of 3.2 °C. The reason for this behavior can be explained by the fact that the natural ventilation provided by opening the windows is effective in releasing the heat accumulation in the interior spaces caused by the direct solar radiation.

(2)　Both the results of PMV and the hourly T_a profiles show that the addition of a corridor in slab blocks could provide effective shading for avoiding excessive solar access and improve the indoor thermal comfort regardless of the windows' status. In comparison, the point and irregular blocks with the centralized plan layout design usually result in the fact that the indoor air temperature and velocity are more sensitive to the façade orientation and the direction of the prevailing wind.

(3)　The results of average wind velocity ratios in various target units confirms that the earlier generations of HDB flats perform better on natural ventilation than the later generations. Nonetheless, this phenomenon cannot be arbitrarily attributed to the change of façade WWR and shading depth. This is because the indoor air velocity is not only affected by these two façade design parameters, but also dependent on the relative sizes of inlet and outlet, as well as the wind direction and facade orientation.

(4)　The linear correlations between the WWR and RETV of façade and average T_a show that these two façade design parameters play important roles in affecting indoor air temperatures. Both the positive impacts of the façade's WWR and RETV on the average T_a were confirmed by OLS regression analysis with a statistical significance at a 0.05 level. It is worth noting that the correlation between RETV and the average T_a in window-closed scenarios is more significant than that in window-open scenarios because opening the windows could change the RETV values.

Although the results of this study have validated that the vertical façade design exerts certain impacts on the indoor air velocity and thermal environment, the combined influencing mechanisms between different façade design parameters are still unclear. In addition, some influential factors on the indoor airflow movement and air temperature are not considered, such as the surrounding buildings, building orientation, room size, window panel and type, and so on. Further investigations are needed before exact conclusions can be drawn. Therefore, it is arbitrary to provide specific values for the façade design parameters due to the above limitations of this study.

To improve the indoor thermal comfort of the HDB flat unit, some principles based on the above conclusions are recommended for the façade design in tropical areas with similar climate conditions. On one hand, larger WWR and limited shading depth could

benefit the indoor natural ventilation while increasing the solar heat gains. So, the WWR and shading depth should be properly designed to be neither too large nor too small to facilitate the natural ventilation and avoid excessive solar heat gains. On the other hand, the lower RETV of the facades could avoid superfluous solar radiations during the daytime. Thus, both the opaque and transparent materials with low RETV are encouraged to be applied. In addition, it is also worth noting that although opening the windows could increase the value of RETV, the indoor thermal environment is significantly improved due to the natural ventilation in comparison to the window-closed scenarios without natural ventilation. Therefore, opening the windows is strongly encouraged for the resident when they are not at home.

Author Contributions: Conceptualization, J.-Y.D. and S.T.; Methodology, J.-Y.D., D.J.C.H. and S.T.; Validation, D.J.C.H.; Investigation, J.-Y.D., Z.Y., E.T. and M.Z.; Data curation, E.T.; Writing—original draft, J.-Y.D.; Writing—review & editing, S.T.; Supervision, N.H.W.; Project administration, N.H.W.; Funding acquisition, N.H.W. All authors have read and agreed to the published version of the manuscript.

Institutional Review Board Statement: Not applicable.

Informed Consent Statement: Not applicable.

Data Availability Statement: Not applicable.

Conflicts of Interest: The authors declare no conflict of interest.

Appendix A. EnergyPlus Simulation Weather Data

Table A1. Weather data of 30 April provided by EnergyPlus.

Hour	Dry-Bulb Temperature (°C)	Wet-Bulb Temperature (°C)	RH (%)	Global Solar Radiation (W/m^2)	Wind Speed (m/s)
1	27	26.21	94	0	0
2	27	25.94	92	0	0
3	27	25.53	89	0	0
4	26	25.22	94	0	0
5	26	25.22	94	0	0
6	26	25.22	94	0	0
7	26	25.22	94	0	0
8	26.5	25.45	92	33	0
9	29	25.99	79	151	1.5
10	30	26.31	75	280	0.5
11	30.2	26.17	73	396	1.5
12	32	24.8	56	496	1.5
13	33	26.23	59	457	2.6
14	33.3	26.3	58	458	1.5
15	33	26.42	60	498	1.9
16	32.8	26.43	61	413	2.2
17	32.5	26.35	62	300	2.6
18	31	26.4	70	158	3.6
19	29.2	26.03	78	38	2
20	28.7	25.86	80	0	0.5
21	28.3	25.78	82	0	0
22	28	25.79	84	0	0
23	27.9	25.83	85	0	0
24	28	25.93	85	0	0

References

1. Department of Statistics Singapore. *M810381-Residents by Age Group & Type of Dwelling, Annual*; Department of Statistics Singapore: Singapore, 2017.
2. Teoalida. Map of HDB Blocks. 2017. Available online: http://www.teoalida.com/singapore/hdbmap/ (accessed on 14 December 2018).
3. Teoalida. HDB Flats Size 1960–2010 Analysis: Are the Flats Shrinking? 2018. Available online: https://www.teoalida.com/singapore/hdbflatsizes/ (accessed on 27 November 2018).
4. Wang, L.; Wong, N.H. The impacts of ventilation strategies and facade on indoor thermal environment for naturally ventilated residential buildings in Singapore. *Build. Environ.* **2007**, *42*, 4006–4015.
5. Givoni, B. Comfort, climate analysis and building design guidelines. *Energy Build.* **1992**, *18*, 11–23. [CrossRef]
6. Givoni, B. *Climate Considerations in Building and Urban Design*; John Wiley & Sons Inc.: New York, NY, USA, 1998.
7. Costanzo, V.; Yao, R.; Xu, T.; Xiong, J.; Zhang, Q.; Li, B. Natural ventilation potential for residential buildings in a densely built-up and highly polluted environment. A case study. *Renew. Energy* **2019**, *138*, 340–353. [CrossRef]
8. Ihm, P.; Krarti, M. Design optimization of energy efficient residential buildings in Tunisia. *Build. Environ.* **2012**, *58*, 81–90. [CrossRef]
9. Jaber, S.; Ajib, S. Thermal and economic windows design for different climate zones. *Energy Build.* **2011**, *43*, 3208–3215. [CrossRef]
10. Eskin, N.; Tuerkmen, H. Analysis of annual heating and cooling energy requirements for office buildings in different climates in Turkey. *Energy Build.* **2008**, *40*, 763–773. [CrossRef]
11. Lam, J.C.; Tsang, C.L.; Li DH, W.; Cheung, S.O. Residential building envelope heat gain and cooling energy requirements. *Energy* **2005**, *30*, 933–951. [CrossRef]
12. Al-Tamimi, N.A.M.; Fadzil, S.F.S.; Harun, W.M.W. The effects of orientation, ventilation, and varied WWR on the thermal performance of residential rooms in the tropics. *J. Sustain. Dev.* **2011**, *4*, 142–149. [CrossRef]
13. Gao, C.F.; Lee, W.L. Evaluating the influence of openings configuration on natural ventilation performance of residential units in Hong Kong. *Build. Environ.* **2011**, *46*, 961–969. [CrossRef]
14. Yoon, N.; Piette, M.A.; Han, J.M.; Wu, W.; Malkawi, A. Optimization of Window Positions for Wind-Driven Natural Ventilation Performance. *Energies* **2020**, *13*, 2464. [CrossRef]
15. Corrado, V.; Serra, V.; Vosilla, A. (Eds.) Performance Analysis of External Shading Devices. In Proceedings of the 30th International Passive and Low Energy Architecture (PLEA) Conference, Ahmedabad, India, 1 January 2004.
16. Al-Tamimi, N.A.; Fadzil, S.F.S. The potential of shading devices for temperature reduction in high-rise residential buildings in the tropics. In Proceedings of the 2011 International Conference on Green Buildings and Sustainable Cities, Bologna, Italy, 15–16 September 2011; Secondini, P., Wu, X., Tondelli, S., Wu, J., Xie, H., Eds.; Elsevier: Amsterdam, The Netherlands, 2011; pp. 273–282.
17. Wong, N.H.; Li, S. A study of the effectiveness of passive climate control in naturally ventilated residential buildings in Singapore. *Build. Environ.* **2007**, *42*, 1395–1405. [CrossRef]
18. Yang, K.H.; Hwang, R.L. Energy conservation of buildings in Taiwan. *Pattern Recognit.* **1995**, *28*, 1483–1491. [CrossRef]
19. Muniz, P.A. The Geometry of External Shading Devices as Related to Natural Ventilation, Daylighting and Thermal Comfort, with Particular Reference to Tropical Hot-Humid Climates. Ph.D. Thesis, Virginia Polytechnic Institute and State University, Blacksburg, VA, USA, 1987.
20. Tzempelikos, A.; Athienitis, A.K. The impact of shading design and control on building cooling and lighting demand. *Sol. Energy* **2007**, *81*, 369–382. [CrossRef]
21. Gratia, E.; De Herde, A. The most efficient position of shading devices in a double-skin facade. *Energy Build.* **2007**, *39*, 364–373. [CrossRef]
22. Cheung, C.K.; Fuller, R.J.; Luther, M.B. Energy-efficient envelope design for high-rise apartments. *Energy Build.* **2005**, *37*, 37–48. [CrossRef]
23. Building and Construction Authority. *Green Mark for Residential Building: 2016 Criteria (GMRB 2016)*; Building and Construction Authority: Singapore, 2016.
24. Energy Market Authority. *Household Energy Consumption, Singapore Energy Statistics 2017*; Energy Market Authority: Singapore, 2017.
25. Moolavi Sanzighi, S.; Soflaei, F.; Shokouhian, M. A comparative study of thermal performance in three generations of Iranian residential buildings: Case studies in Csa Gorgan. *J. Build. Phys.* **2020**, *44*, 326–363. [CrossRef]
26. Meteorological Service Singapore. *Climate of Singapore, 2020*; Meteorological Service Singapore (MSS): Singapore, 2020. Available online: http://www.weather.gov.sg/climate-climate-of-singapore/ (accessed on 1 September 2020).
27. National Environment Agency. Sunshine Duration- Monthly Mean Daily Duration: National Environment Agency. 2020. Available online: https://data.gov.sg/dataset/sunshine-duration-monthly-mean-daily-duration (accessed on 1 September 2020).
28. Blocken, B. Computational Fluid Dynamics for urban physics: Importance, scales, possibilities, limitations and ten tips and tricks towards accurate and reliable simulations. *Build. Environ.* **2015**, *91*, 219–245. [CrossRef]
29. Tominaga, Y.; Mochida, A.; Yoshie, R.; Kataoka, H.; Nozu, T.; Yoshikawa, M.; Shirasawa, T. AIJ guidelines for practical applications of CFD to pedestrian wind environment around buildings. *J. Wind. Eng. Ind. Aerodyn.* **2008**, *96*, 1749–1761. [CrossRef]
30. Franke, J.; Hellsten, A.; Schluenzen, K.H.; Carissimo, B. The COST 732 Best Practice Guideline for CFD simulation of flows in the urban environment: A summary. *Int. J. Environ. Pollut.* **2011**, *44*, 419–427. [CrossRef]
31. Richards, P.J.; Hoxey, R.P. Appropriate boundary conditions for computational wind engineering models using the k-ε turbulence model. In *Computational Wind Engineering 1*; Murakami, S., Ed.; Elsevier: Oxford, UK, 1993; pp. 145–153.
32. Launder, B.E.; Spalding, D.B. The numerical computation of turbulent flows. *Comput. Methods Appl. Mech. Eng.* **1974**, *3*, 269. [CrossRef]

33. Cebeci, T.; Bradshaw, P. *Momentum Transfer in Boundary Layers*; Hemisphere Publishing Corporation: New York, NY, USA, 1977.
34. Shih, T.-H.; Liou, W.W.; Shabbir, A.; Yang, Z.; Zhu, J. A new k-ϵ eddy viscosity model for high reynolds number turbulent flows. *Comput. Fluids* **1995**, *24*, 227–238. [CrossRef]
35. Franke, J.; Hirsch, C.; Jensen, A.G.; Krüs, H.W.; Schatzmann, M.; Westbury, P.S.; Miles, S.D.; Wisse, J.A.; Wright, N.G. (Eds.) Recommendations on the use of CFD in wind engineering. In Proceedings of the International Conference on Urban Wind Engineering and Building Aerodynamics, Sint-Genesius-Rode, Belgium, 5–7 May 2004.
36. Linden, P.F. The fluid mechanics of natural ventilation. *Annu. Rev. Fluid Mech.* **1999**, *31*, 201–238. [CrossRef]
37. Sorensen, D.N.; Nielsen, P.V. Quality control of computational fluid dynamics in indoor environments. *Indoor Air* **2003**, *13*, 2–17. [CrossRef] [PubMed]
38. Ramponi, R.; Blocken, B. CFD simulation of cross-ventilation for a generic isolated building: Impact of computational parameters. *Build. Environ.* **2012**, *53*, 34–48. [CrossRef]
39. Karava, P.; Stathopoulos, T.; Athienitis, A.K. Airflow assessment in cross-ventilated buildings with operable facade elements. *Build. Environ.* **2011**, *46*, 266–279. [CrossRef]
40. Wang, L.; Wong Nyuk, H.; Li, S. Facade design optimization for naturally ventilated residential buildings in Singapore. *Energy Build.* **2007**, *39*, 954–961. [CrossRef]
41. Fung, Y.W.; Lee, W.L. Identifying the most influential parameter affecting natural ventilation performance in high-rise high-density residential buildings. *Indoor Built Environ.* **2015**, *24*, 803–812. [CrossRef]
42. Heiselberg, P.; Sandberg, M. Evaluation of discharge coefficients for window openings in wind driven natural ventilation. *Int. J. Vent.* **2006**, *5*, 43–52. [CrossRef]
43. Heiselberg, P.; Bjørn, E.; Nielsen, P.V. Impact of open windows on room air flow and thermal comfort. *Int. J. Vent.* **2002**, *1*, 91–100. [CrossRef]